Chemical Vapor Deposition and Etching of High-Quality Monolayer Hexagonal Boron Nitride Films

Peter Sutter,* Jayeeta Lahiri, Peter Albrecht, and Eli Sutter

Center for Functional Nanomaterials, Brookhaven National Laboratory, Upton, New York 11973, United States

ABSTRACT The growth of large-area hexagonal boron nitride (h-BN) monolayers on catalytic metal substrates is a topic of scientific and technological interest. We have used real-time microscopy during the growth process to study h-BN chemical vapor deposition (CVD) from borazine on Ru(0001) single crystals and thin films. At low borazine pressures, individual h-BN domains nucleate sparsely, grow to macroscopic dimensions, and coalescence to form a closed monolayer film. A quantitative analysis shows borazine adsorption and dissociation predominantly on Ru, with the h-BN covered areas being at least 100 times less reactive. We establish strong effects of hydrogen added to the CVD precursor gas in controlling the in-plane expansion and morphology of the growing h-BN domains. High-temperature exposure of h-BN/Ru to pure hydrogen causes the controlled edge detachment of B and N and can be used as a clean etching process for h-BN on metals.

KEYWORDS: boron nitride · monolayer films · growth · etching · borazine · hydrogen · transition metal

The successful isolation of free-standing two-dimensional (2D) crystals[1] has opened up avenues for producing 2D membranes of a variety of materials and for creating new engineered materials with unique functional properties by assembling heterostructures that consist of stacks of atomically thin membranes. So far, most attention has focused on graphene, a 2D sheet of sp^2-bonded carbon atoms, which has shown a range of interesting electronic,[2,3] mechanical,[4] and chemical[5] properties. Synthesis methods for graphene with quality approaching that required for large-scale applications have recently been developed.[6−10] To access other 2D materials and ultimately realize the vision of "materials on demand" by stacking of graphene and other atomically thin membranes, scalable synthesis methods need to be developed for other systems, such as hexagonal boron nitride (h-BN), molybdenum disulfide (MoS_2), niobium diselenide ($NbSe_2$), *etc.*

Among the known 2D materials, h-BN—an electrical insulator isostructural with graphene—has attracted particular interest due to the recognition that heterostructures of graphene with h-BN could provide enhanced functionality. Graphene devices supported on h-BN films, for instance, have shown very high carrier mobilities approaching those of suspended graphene.[11] Calculations have predicted spin-polarized transport near in-plane graphene/h-BN junctions,[12] and finally, seamlessly attached bands of h-BN may enable a more stable passivation of the edges of graphene nanostructures than the hydrogen passivation invoked in theoretical models.[13] The emerging applications of h-BN in combination with graphene call for methods for producing high-quality h-BN films, whose development in turn requires an understanding of fundamental BN growth mechanisms. "Nanomesh" structures of h-BN on different transition metal surfaces, including Rh(111)[14] and Ru(0001),[15] have been prepared by chemical vapor deposition (CVD) using borazine $(HBNH)_3$ for applications as ordered templates for the adsorption of molecules[14,16] and metal nanoparticles.[15,17] While a nanomesh results from varying local registries between a metal substrate and the h-BN film in a commensurate or incommensurate superstructure (*i.e.*, a moiré), a similar CVD process could be used to produce high-quality free-standing h-BN membranes if the growth is carried out on a sacrificial metal substrate that can subsequently be etched away, analogous to the procedure used to isolate graphene from metal films or foils.[6,7,10,18] Following a general approach of this type, large-area few-layer h-BN membranes with thickness between two and five atomic layers have been synthesized recently by ammonia−borane CVD on Cu foils.[19]

Here, we use real-time low-energy electron microscopy (LEEM) during CVD growth to study key aspects of the synthesis of high-quality h-BN monolayers on transition

* Address correspondence to psutter@bnl.gov.

Received for review June 10, 2011 and accepted July 27, 2011.

Published online July 27, 2011
10.1021/nn202141k

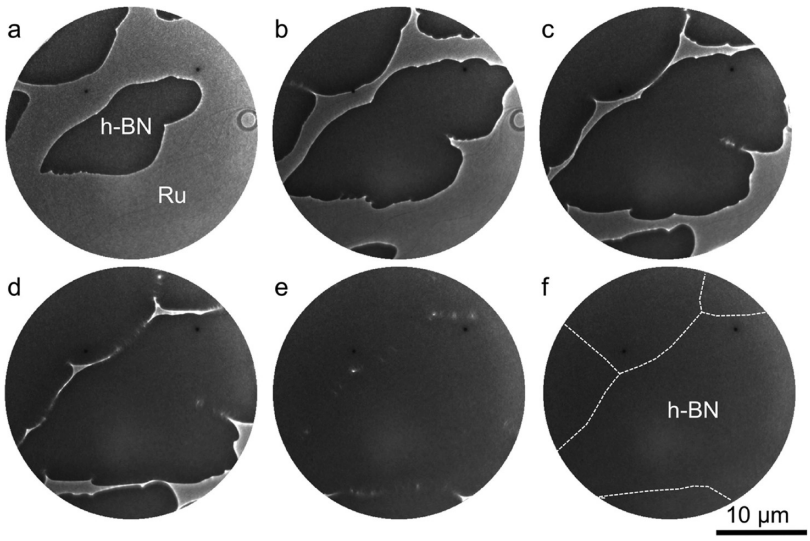

Figure 1. Macroscopic h-BN domains on Ru(0001) obtained by CVD growth from borazine. (a–f) LEEM images at different growth stages to the full coalescence of the h-BN monolayer. Temperature = 780 °C; borazine pressure = 1.3 × 10^{-8} Torr; elapsed time = (a) 0, (b) 300 s, (c) 600 s, (d) 900 s, (e) 1200 s, (f) 1350 s. (f) Complete coalescence is achieved. Dashed lines mark the final domain boundaries, traced from (e).

metal substrates. Our results show that at low precursor pressures (*i.e.*, small B and N supersaturation) individual h-BN domains nucleate sparsely and can grow to large sizes of at least tens of micrometers, thus minimizing the number of defects associated with domain boundaries in coalesced monolayer films covering the entire substrate area (~1 cm^2 in our case). A quantitative analysis shows that the growth proceeds predominantly *via* adsorption on the exposed metal surface and hence self-terminates at one atomic layer thickness. Finally, we elucidate the role of growth modifiers, such as mixtures of the BN precursor gas with other gases, in manipulating the growth process to achieve well-ordered and large h-BN domains with controllable shape. In combination with other *in situ* and *ex situ* characterization, our real-time surface microscopy study shows that CVD growth on transition metal substrates is a viable method for producing high-quality h-BN monolayers and provides insight into factors by which the growth process can be controlled.

Figure 1 shows still images extracted from a LEEM movie of h-BN growth during the exposure of Ru(0001) to borazine at 780 °C, following the initial h-BN nucleation in a mixture of borazine and H_2, which is discussed in more detail below. Low borazine pressures (10^{-8} Torr or below) lead to a very sparse nucleation of h-BN domains, spaced tens of micrometers apart, similar to the nucleation of graphene on Ru(0001) at low carbon supersaturation.[8] Considering the density of surface steps on the metal substrate, visible as faint dark lines in the exposed Ru areas (*e.g.*, in Figure 1a), we find that the h-BN domains readily grow to sizes exceeding the step spacing by at least 2 orders of magnitude. Large h-BN domains grow across Ru steps continuously and without secondary nucleation events; that is, h-BN shows the same carpet-like edge flow across substrate steps found previously for graphene on different metal substrates (*e.g.*, Ru(0001),[8] Ir(111),[20] Pt(111)[21]). This finding is in contrast to earlier conclusions, based on scanning tunneling microscopy (STM) on disordered h-BN layers on Ru(0001), that h-BN cannot flow continuously across steps on Ru(0001).[15] Within our image resolution, we do not observe any motion of the Ru step edges; that is, the h-BN growth is not accompanied by significant changes in the surface morphology of the substrate.

Continued exposure to borazine leads to the growth and ultimately coalescence of the large h-BN domains. Given the lattice mismatch between h-BN and Ru(0001), and the resulting formation of a moiré structure in which 13 × 13 h-BN units are matched to 12 × 12 surface unit cells of Ru with rotationally aligned BN and Ru surface meshes (see below), any two h-BN domains will likely exhibit a random in-plane shift and could form a line defect upon coalescence.[22] The only way of minimizing such defects is by maximizing the spacing and, hence, the final size of the individual domains. The successful growth of macroscopic domains, as shown in Figure 1, demonstrates that low precursor pressures make this feasible for h-BN on transition metals. The generality of this finding is underscored by a recent STM study, which suggested that in h-BN CVD from borazine on a different transition metal, Rh(111), low precursor pressures are required to achieve high-quality h-BN films with minimal density of domain boundaries.[22]

The time-dependent 2D growth rate of h-BN, determined from real-time microscopy, can be used to analyze important growth characteristics and provide a foundation for optimizing this approach to synthesizing h-BN monolayers. Figure 2 shows the time

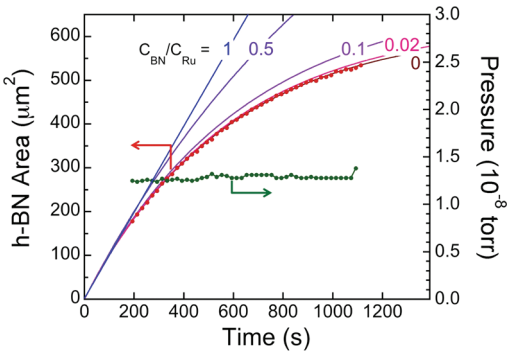

Figure 2. Analysis of h-BN growth rate during CVD growth from borazine. Time-dependent h-BN coverage at constant borazine pressure, determined from the LEEM movie in Figure 1. Dots: experimental data. Lines: modeling of the data, assuming different ratios C_{BN}/C_{Ru} of the borazine growth coefficient on h-BN covered and exposed parts of the Ru substrate. The best fit to the data is achieved for $C_{BN}/C_{Ru} = 0$, *i.e.*, assuming completely inert h-BN.

evolution of the h-BN coverage within a fixed field of view at constant borazine pressure. The area covered by h-BN increases sublinearly with time; that is, the growth rate is progressively reduced as the h-BN coverage increases. CVD growth processes involve four distinct steps: (i) the adsorption of molecules of a precursor gas on the surface with sticking coefficient S; (ii) the decomposition of the precursor and formation of mobile surface species; (iii) diffusion of these species; and (iv) nucleation and/or incorporation into the growing film, here h-BN. As the surface becomes progressively covered by h-BN, there will be two complementary surface regions—bare Ru metal and Ru covered by h-BN—that may contribute to different degrees to the continued h-BN growth *via* steps i–iii.

Given the expected large difference in reactivity between Ru and the relatively inert h-BN surface, the most likely reason for the observed slowing of the h-BN growth is a progressive reduction in the area of active Ru, where borazine can adsorb and decompose efficiently.[23] To corroborate this scenario, we have fitted the experimental growth curve to a model assuming different dissociative sticking coefficients of Ru and of h-BN domains, quantified by the ratio S_{BN}/S_{Ru}. The rate of change of the h-BN covered area, A, in a fixed field of view (area A_{FOV}) due to the supply of B and N atoms from Ru and h-BN is given by

$$\frac{dA}{dt} = C_{Ru}(A_{FOV} - A) + C_{BN}A \qquad (1)$$

where $C_{Ru,BN}$ are growth constants proportional to the borazine sticking coefficients on Ru and h-BN, respectively. Solving eq 1 results in

$$A(t) = A_{FOV}\frac{C_{Ru}}{C_{Ru} - C_{BN}} \times [1 - e^{-(C_{Ru} - C_{BN})t}] \qquad (2)$$

The best fit to the experimentally determined h-BN growth, $A(t)$, is obtained by assuming that the h-BN domains are completely inert, that is, do not contribute to the formation of mobile N- and B-containing surface species, whereas borazine adsorbed and decomposed on free Ru provides a constant amount of these species per unit area and time. Plots of eq 2 for different ratios of the growth constants, C_{BN}/C_{Ru}, shown as solid lines in Figure 2, allow us to establish an upper bound $C_{BN}/C_{Ru} < 0.01$. From this analysis, we conclude that h-BN growth from borazine on Ru(0001) proceeds by a 2D CVD process, in which the precursor adsorbs and dissociates predominantly on areas of exposed metal. Conversely, the already h-BN covered areas do not contribute any measurable amounts of B and N to the further growth. This can have different reasons: borazine could adsorb and dissociate, but the mass transport of the adsorbed species to the growing h-BN edge could be hindered by high diffusion or edge-crossing barriers. Also, the binding energy for borazine at our high growth temperatures could be too weak, so that any adsorbed precursor molecules rapidly desorb back into the gas phase. The finding in our work, as well as previous studies, that STM on h-BN films after cooling to room temperature does not show any adsorbed borazine or dissociated fragments provides strong support for the latter scenario, that is, the weak binding (*i.e.*, small sticking coefficient $S_{h\text{-}BN}$) of borazine molecules on h-BN at the growth temperature. The growing h-BN film essentially constitutes an inert blanket that masks a progressively larger fraction of the surface during growth, and the h-BN thickness will therefore self-terminate at one atomic layer, at least for sufficiently small precursor pressures.[24] This self-termination of the h-BN growth from borazine appears to be a general phenomenon for different transition metal surfaces, and similar conclusions have been reached for h-BN growth on Pt(111)[23] and Ni(111).[25] Knowledge of the active phase for borazine adsorption and decomposition can be used to predict important aspects of the growth process. As an example, our results show that the borazine partial pressure needs to be increased exponentially with time to achieve a constant h-BN growth rate.

To evaluate the structure and morphology of h-BN monolayers with macroscopic domain sizes on Ru(0001), we have performed STM and low-energy electron diffraction (LEED), as shown in Figure 3. Large-scale STM images show continuous h-BN domains with a "nanomesh" moiré structure,[26] similar to that of h-BN/Rh(111),[14] confirming single atomic layer thickness. In contrast to previous results for h-BN/Ru(0001), which showed considerable disorder, the films achieved here appear structurally perfect and show a very low defect density. LEED confirms the hexagonal structure of the h-BN monolayer and has been used to analyze the moiré structure between h-BN (surface lattice constant = 2.50 Å) and Ru(0001) (2.71 Å). We find a coincidence

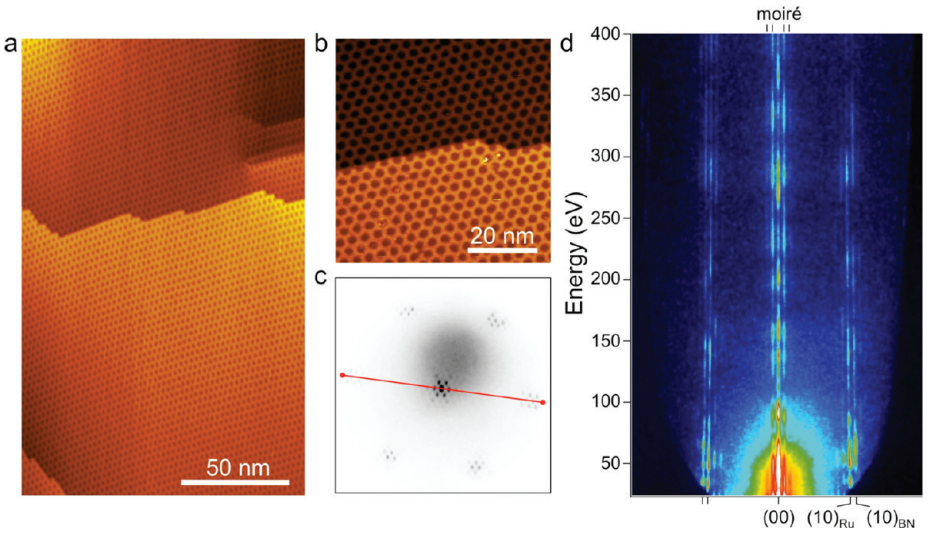

Figure 3. Characterization of h-BN on Ru(0001). (a) UHV STM overview scan of a h-BN film on a Ru(0001) thin film, grown epitaxially on sapphire (0001). The image shows a moiré pattern (nanomesh) with very low defect density. (b) Zoomed-in view of the moiré across a Ru surface step. (c) LEED (E = 40 eV) showing multiple diffraction orders of the h-BN/Ru(0001) moiré structure. (d) LEED $I(V)$ data (25 eV < E < 400 eV) along the red line in (c).

structure with 13 × 13 h-BN unit cells matched to 12 × 12 units of Ru (residual misfit strain <0.1%), in agreement with previous results.[15,23] Importantly, diffraction data obtained across our entire samples show perfect rotational alignment of the $\langle 10\bar{1}0 \rangle$ in-plane directions of the h-BN layer and Ru substrate, which is consistent with a strong interaction between h-BN and Ru[27] and implies a uniform h-BN lattice orientation and the absence of finite-angle domain boundaries over large sample areas.

CVD growth is frequently performed in mixtures of the active growth precursor with an additional "carrier" or "forming" gas. Reactive gases such as H_2 are used in an attempt to achieve highly reducing conditions and suppress the formation of surface oxides on metal substrates. In recent CVD growth of h-BN on Cu, for instance, Ar/H_2 was mixed with the growth precursor.[19] We used *in situ* observations to explore the microscopic effects of hydrogen on the h-BN growth. Numerous experiments on the formation of h-BN on Ru have shown that the h-BN CVD growth from borazine is surprisingly sensitive to small changes in the gas composition, as illustrated in Figure 4. The growth of h-BN on Ru(0001) from undiluted, high-purity borazine typically proceeds highly anisotropically (Figure 4a–c) and is strongly influenced by the atomic step structure of the metal substrate. The h-BN edge flow in the direction parallel to surface steps is substantially faster than the growth across steps, indicative of a hindered step-crossing by the h-BN domains. Figure 4c illustrates that the domain expansion is nearly suppressed both in the uphill and downhill directions but proceeds at high rate along the steps, thus producing a high-density of anisotropic, wire-like h-BN domains closely following Ru

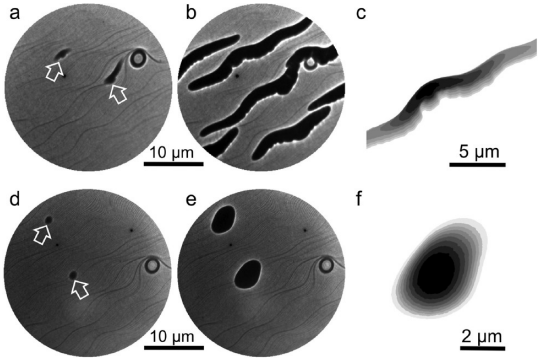

Figure 4. Effect of growth modifiers (here H_2) on h-BN CVD on Ru(0001). (a,b) LEEM images showing the h-BN morphology during growth from borazine [$p = 7 \times 10^{-9}$ Torr]. (c) Time evolution of a single h-BN domain: fast growth along the Ru(0001) step direction; slow growth across substrate steps. Time increment: 5 s. Darker shades of gray correspond to earlier times. (d,e) LEEM images showing the h-BN morphology during growth in a mixture of borazine and H_2 (1:10; $p_{tot} = 7 \times 10^{-8}$ Torr). (f) Time evolution of a single h-BN domain: compact domain shape; nearly isotropic growth along and across substrate steps. Time increment: 5 s. Darker shades of gray correspond to earlier times.

surface steps. Figure 4d–f shows a similar growth experiment in the same sample area but with concurrent exposure to borazine and H_2 (ratio 1:10). Compared to the growth in borazine alone, the h-BN nucleation density is reduced, the individual domains grow more slowly, and they assume compact shapes with nearly isotropic edge flow rate irrespective of the underlying Ru step structure.

Given that the dissociation of borazine to B and N liberates 6 H atoms per $(HBNH)_3$ molecule, the distinct modification of h-BN growth by H_2, making available a mere 20 additional H atoms per borazine unit (at a ratio of 1:10) is quite striking. Several possible factors could

contribute to the change in growth behavior with the addition of H_2. The reduction of residual surface oxygen decorating the Ru step edges or a modification of the electronic structure of the Ru surface steps by hydrogen adsorption could facilitate the carpet-like flow of h-BN domains across steps. In particular, the step-crossing of the h-BN domains in the uphill direction, not observed in the growth from pure borazine (Figure 4a), appears significantly enhanced in the presence of additional H_2 (Figure 4b). While in the growth from borazine alone, the Ru steps completely suppress h-BN edge flow in the uphill direction, the addition of H_2 leads to nearly identical step-crossing rates in the uphill and downhill directions. Another possibility is a hydrogen-induced modification of the diffusion of the mobile surface species, changing the relative diffusion rates of dissociated borazine fragments on the terraces, along Ru steps, and across steps. Predominant diffusion along steps could explain the highly anisotropic growth from pure borazine (Figure 4a), leading to ratios of the rate $R_{\parallel}$ of expansion along the Ru step directions to the rate $R_{\perp}$ perpendicular to the steps exceeding 25. With the addition of H_2, the h-BN edge flow becomes nearly isotropic (Figure 4b), with ratio $R_{\parallel}/R_{\perp} \approx 1.5$.

Two particular characteristics, the reduced h-BN nucleation density and the overall slower h-BN growth in the mixed atmosphere, suggest additional, more complex effects of H_2, possibly a slowing of the edge incorporation or even a direct attack of the h-BN edge by H atoms generated by H_2 dissociation on the transition metal surface. To further explore this possibility, we have performed real-time microscopy experiments on the interaction of atomic H with metal-supported 2D h-BN domains. To maximize the rates of any hydrogen-induced effects, we employed the direct exposure to atomic H generated by a cracker source. Control experiments using exposure to molecular hydrogen showed the same qualitative behavior, albeit at reduced rate. Figure 5 illustrates the response of compact h-BN domains with sizes of several square micrometers on Ru(0001) to atomic H exposure at 700 °C. No modifications are detectable on the metal surface; the h-BN domains, however, shrink continuously by reverse edge flow and ultimately disappear completely. We note that the same domains were stable over long times when held at this temperature in ultrahigh vacuum (UHV) but experienced similar (but slower) etching during exposure to H_2. We conclude that atomic H, either dosed directly or generated by dissociation of H_2 on Ru(0001), can etch h-BN edges.

From the LEEM movie of Figure 5, we have measured the time-dependent area of individual h-BN domains, $A(t)$, during etching by atomic H (Figure 5e). The elementary steps involved in the H etching process are the H-assisted detachment of B and N from the h-BN edge, followed by either a direct desorption of the

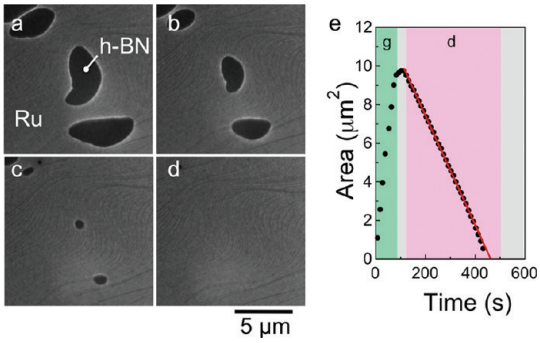

Figure 5. Etching of h-BN domains by hydrogen exposure. (a–d) LEEM images showing the h-BN morphology during exposure to atomic H [$p(H_2) = 1.5 \times 10^{-7}$ Torr; elapsed time = (a) 0, (b) 240 s, (c) 350 s, (d) 380 s]. (e) Measured area of a single h-BN domain during exposure to borazine [growth (green); $p = 10^{-8}$ Torr] and atomic H [decay (red); $p(H_2) = 1.5 \times 10^{-7}$ Torr].

hydrated BH_x and NH_x (and possibly mixed BNH_x) species from the edge or a sequence of surface diffusion away from the h-BN edge and desorption from the Ru surface. The microscopic steps as well as the overall driving force—a difference in chemical potential between the initial and final states—are closely analogous to those in the well-studied phenomenon of Ostwald ripening on single-crystal surfaces,[28] the primary difference being the nature of the final state (surface bound in ripening; desorbed in the gas phase in etching). Hence, we can use the framework of surface Ostwald ripening[28] and of ripening processes assisted by adsorbates[29] to identify the likely rate-limiting step of the H-induced etching of h-BN domains on Ru(0001). The signature for different rate-limiting steps lies in the time dependence of the h-BN domain area, $A(t)$. When an ample supply of atomic H is assumed, given in our direct dosing experiments, a power-law dependence $A(t) \sim (t_0 - t)^{2/3}$, with t_0 denoting the time of disappearance of the domain, would indicate a diffusion-limited h-BN domain decay; for $A(t) \sim (t_0 - t)$, on the other hand, the detachment from the domain edge is the rate-limiting process. Our observations clearly show $A(t) \sim (t_0 - t)$ (Figure 5e), that is, detachment-limited kinetics of the H etching process. Since the h-BN domains are stable in UHV at the same temperature, we conclude that H promotes the edge detachment of both B and N, likely *via* BH_x and NH_x intermediates that can desorb at high temperature.[30,31] While hydrogen exposure can serve as a potent growth modifier during h-BN CVD on metals (Figure 4), H-induced edge detachment processes can be used for etching h-BN films (Figure 5), that is, as an alternative to the known oxygen etching of h-BN,[32] with the advantage of not involving O that binds very strongly on most transition metal surfaces.[33]

Our real-time microscopy experiments on a specific model system—h-BN monolayers on Ru(0001)—provide evidence for the feasibility of synthesizing

large monocrystalline h-BN domains on transition metal templates. CVD growth on Ru(0001) at temperatures near 800 °C and at low borazine pressures produces sparse arrays of h-BN nuclei, which grow to macroscopic dimensions and coalesce to a closed film of very high crystal quality covering the entire sample surface. Experiments on the use of a simple growth modifier, additional H_2 mixed with the borazine precursor, provide evidence that the B and N incorporation at the h-BN edge can be tuned to control the growth and achieve h-BN domains with different morphology. Exposure to hydrogen alone, finally, is found to reverse the growth process and etch macroscopic h-BN domains. Observed on both Ru(0001) single crystals and epitaxial Ru(0001) thin films on sapphire, these growth and processing mechanisms pave the way for the fabrication of free-standing h-BN membranes by growth on sacrificial Ru templates.[10] It should be possible to achieve similar domain sizes and control over h-BN CVD growth, as well as hydrogen-induced growth modifications and h-BN etching, on a wide range of other metals with catalytic properties similar to Ru, including for instance Ni thin films[6,18] and Cu foils.[7] Comparison of low-pressure borazine CVD with other synthesis concepts, such as a three-step process involving sequential deposition of B and N demonstrated recently on Rh(111) thin films,[34] will be necessary to identify—for example by real-time surface microscopy as used here—the optimal approach for producing high-quality h-BN monolayers with the largest possible domain size.

METHODS

We have used real-time microscopy during the growth and processing of h-BN on Ru(0001) single crystals and epitaxial Ru(0001) thin films on sapphire substrates. Ru single-crystal surfaces were prepared by the standard method, involving several cycles of oxygen adsorption and flashing to temperatures above 1500 °C. Epitaxial Ru thin films were grown by magnetron sputtering on *c*-axis oriented sapphire substrates, as described previously.[10] The h-BN growth was performed in ultrahigh vacuum (UHV) by exposure of the metal surface to high-purity borazine at high temperatures. Additional H_2 gas (research purity, 99.999%) was dosed in some of the experiments to establish the resulting effects on the growth process. H-induced modifications to as-grown h-BN monolayers on Ru were probed by cracking H_2 using a high-efficiency atomic-H doser. In describing these experiments, we state the pressure of background H_2 in the chamber during H exposure. Bright-field low-energy electron microscopy (LEEM) and Hg lamp excited photoelectron microscopy (PEEM) in an Elmitec LEEM V field-emission microscope were employed to observe h-BN growth and processing in real time. Sample temperatures were measured using a W–Re thermocouple spot-welded onto the metal sample support. The structure and ordering of the CVD-grown h-BN films were characterized by selected-area low-energy electron diffraction (micro-LEED) in the LEEM instrument and by room temperature scanning tunneling microscopy (STM) in a separate UHV system with *in situ* growth capability. The h-BN films imaged by STM were synthesized using processes identical to those in our real-time LEEM investigation.

Acknowledgment. This research has been carried out at the Center for Functional Nanomaterials, Brookhaven National Laboratory, which is supported by the U.S. Department of Energy, Office of Basic Energy Sciences, under Contract No. DE-AC02-98CH10886.

REFERENCES AND NOTES

1. Novoselov, K. S.; Jiang, D.; Schedin, F.; Booth, T. J.; Khotkevich, V. V.; Morozov, S. V.; Geim, A. K. Two-Dimensional Atomic Crystals. *Proc. Natl. Acad. Sci. U.S.A.* **2005**, *102*, 10451–10453.
2. Novoselov, K. S.; Geim, A. K.; Morozov, S. V.; Jiang, D.; Zhang, Y.; Dubonos, S. V.; Grigorieva, I. V.; Firsov, A. A. Electric Field Effect in Atomically Thin Carbon Films. *Science* **2004**, *306*, 666–669.
3. Zhang, Y.; Tan, J. W.; Stormer, H. L.; Kim, P. Experimental Observation of the Quantum Hall Effect and Berry's Phase in Graphene. *Nature* **2005**, *438*, 201–204.
4. Lee, C.; Wei, X.; Kysar, J. W.; Hone, J. Measurement of the Elastic Properties and Intrinsic Strength of Monolayer Graphene. *Science* **2008**, *321*, 385–388.
5. Schedin, F.; Geim, A. K.; Morozov, S. V.; Hill, E. W.; Blake, P.; Katsnelson, M. I.; Novoselov, K. S. Detection of Individual Gas Molecules Adsorbed on Graphene. *Nat. Mater.* **2007**, *6*, 652–655.
6. Reina, A.; Jia, X.; Ho, J.; Nezich, D.; Son, H.; Bulovic, V.; Dresselhaus, M. S.; Kong, J. Large Area, Few-Layer Graphene Films on Arbitrary Substrates by Chemical Vapor Deposition. *Nano Lett.* **2009**, *9*, 30–35.
7. Li, X.; Cai, W.; An, J.; Kim, S.; Nah, J.; Yang, D.; Piner, R.; Velamakanni, A.; Jung, I.; Tutuc, E.; *et al.* Large-Area Synthesis of High-Quality and Uniform Graphene Films on Copper Foils. *Science* **2009**, *324*, 1312–1314.
8. Sutter, P. W.; Flege, J.-I.; Sutter, E. A. Epitaxial Graphene on Ruthenium. *Nat. Mater.* **2008**, *7*, 406–411.
9. Emtsev, K. V.; Bostwick, A.; Horn, K.; Jobst, J.; Kellogg, G. L.; Ley, L.; McChesney, J. L.; Ohta, T.; Reshanov, S. A.; Rohrl, J.; *et al.* Towards Wafer-Size Graphene Layers by Atmospheric Pressure Graphitization of Silicon Carbide. *Nat. Mater.* **2009**, *8*, 203–207.
10. Sutter, P. W.; Albrecht, P. M.; Sutter, E. A. Graphene Growth on Epitaxial Ru Thin Films on Sapphire. *Appl. Phys. Lett.* **2010**, *97*, 213101.
11. Dean, C. R.; Young, A. F.; Meric, I.; Lee, C.; Wang, L.; Sorgenfrei, S.; Watanabe, K.; Taniguchi, T.; Kim, P.; Shepard, K. L.; *et al.* Boron Nitride Substrates for High-Quality Graphene Electronics. *Nat. Nanotechnol.* **2010**, *5*, 722–726.
12. Pruneda, J. M. Origin of Half-Semimetallicity Induced at Interfaces of C-BN Heterostructures. *Phys. Rev. B* **2010**, *81*, 161409.
13. Wang, Z. F.; Li, Q.; Zheng, H.; Ren, H.; Su, H.; Shi, Q. W.; Chen, J. Tuning the Electronic Structure of Graphene Nanoribbons through Chemical Edge Modification: A Theoretical Study. *Phys. Rev. B* **2007**, *75*, 113406.
14. Corso, M.; Auwarter, W.; Muntwiler, M.; Tamai, A.; Greber, T.; Osterwalder, J. Boron Nitride Nanomesh. *Science* **2004**, *303*, 217–220.
15. Goriachko, A.; He; Knapp, M.; Over, H.; Corso, M.; Brugger, T.; Berner, S.; Osterwalder, J.; Greber, T. Self-Assembly of a Hexagonal Boron Nitride Nanomesh on Ru(0001). *Langmuir* **2007**, *23*, 2928–2931.
16. Berner, S.; Corso, M.; Widmer, R.; Groening, O.; Laskowski, R.; Blaha, P.; Schwarz, K.; Goriachko, A.; Over, H.; Gsell, S.; *et al.* Boron Nitride Nanomesh: Functionality from a Corrugated Monolayer. *Angew. Chem.* **2007**, *119*, 5207–5211.

17. Zhang, J.; Sessi, V.; Michaelis, C. H.; Brihuega, I.; Honolka, J.; Kern, K.; Skomski, R.; Chen, X.; Rojas, G.; Enders, A. Ordered Layers of Co Clusters on BN Template Layers. *Phys. Rev. B* **2008**, *78*, 165430.
18. Kim, K. S.; Zhao, Y.; Jang, H.; Lee, S. Y.; Kim, J. M.; Kim, K. S.; Ahn, J.-H.; Kim, P.; Choi, J.-Y.; Hong, B. H. Large-Scale Pattern Growth of Graphene Films for Stretchable Transparent Electrodes. *Nature* **2009**, *457*, 706–710.
19. Song, L.; Ci, L.; Lu, H.; Sorokin, P. B.; Jin, C.; Ni, J.; Kvashnin, A. G.; Kvashnin, D. G.; Lou, J.; Yakobson, B. I.; *et al.* Large Scale Growth and Characterization of Atomic Hexagonal Boron Nitride Layers. *Nano Lett.* **2010**, *10*, 3209–3215.
20. Coraux, J.; N'Diaye, A. T.; Busse, C.; Michely, T. Structural Coherency of Graphene on Ir(111). *Nano Lett.* **2008**, *8*, 565–570.
21. Sutter, P.; Sadowski, J. T.; Sutter, E. Graphene on Pt(111): Growth and Substrate Interaction. *Phys. Rev. B* **2009**, *80*, 245411.
22. Dong, G.; Fourre, E. B.; Tabak, F. C.; Frenken, J. W. M. How Boron Nitride Forms a Regular Nanomesh on Rh(111). *Phys. Rev. Lett.* **2010**, *104*, 096102.
23. Paffettt, M. T.; Simonson, R. J.; Papin, P.; Paine, R. T. Borazine Adsorption and Decomposition at Pt(111) and Ru(001) Surfaces. *Surf. Sci.* **1990**, *232*, 286–296.
24. Previous reports of Stranski–Krastanov-type multilayer h-BN growth on Ni(111) (ref 25) and recent observations that growth at atmospheric pressure on Cu foils produces few-layer h-BN films (ref 19) suggest a low residual reactivity of h-BN on transition metals, sufficient to provide small amounts of N- and B-containing species for multilayer growth at very high precursor doses.
25. Nagashima, A.; Tejima, N.; Gamou, Y.; Kawai, T.; Oshima, C. Electronic Dispersion Relations of Monolayer Hexagonal Boron Nitride Formed on the Ni(111) Surface. *Phys. Rev. B* **1995**, *51*, 4606–4613.
26. Laskowski, R.; Blaha, P. *Ab Initio* Study of h-BN Nanomeshes on Ru(001), Rh(111), and Pt(111). *Phys. Rev. B* **2010**, *81*, 075418.
27. Preobrajenski, A. B.; Nesterov, M. A.; Ng, M. L.; Vinogradov, A. S.; Martensson, N. Monolayer h-BN on Lattice-Mismatched Metal Surfaces: On the Formation of the Nanomesh. *Chem. Phys. Lett.* **2007**, *446*, 119–123.
28. Giesen, M. Step and Island Dynamics at Solid/Vacuum and Solid/Liquid Interfaces. *Prog. Surf. Sci.* **2001**, *68*, 1–154.
29. Thiel, P. A.; Shen, M.; Liu, D.-J.; Evans, J. W. Adsorbate-Enhanced Transport of Metals on Metal Surfaces: Oxygen and Sulfur on Coinage Metals. *J. Vac. Sci. Technol., A* **2010**, *28*, 1285–1298.
30. Logadottir, A.; Norskov, J. K. Ammonia Synthesis over a Ru(0001) Surface Studied by Density Functional Calculations. *J. Catal.* **2003**, *220*, 273–279.
31. Rauscher, H.; Kostov, K. L.; Menzel, D. Adsorption and Decomposition of Hydrazine on Ru(001). *Chem. Phys.* **1993**, *177*, 473–496.
32. Goriachko, A.; Zakharov, A. A.; Over, H. Oxygen-Etching of h-BN/Ru(0001) Nanomesh on the Nano- and Mesoscopic Scale. *J. Phys. Chem. C* **2008**, *112*, 10423–10427.
33. Stampfl, C.; Schwegmann, S.; Over, H.; Scheffler, M.; Ertl, G. Structure and Stability of a High-Coverage (1×1) Oxygen Phase on Ru(0001). *Phys. Rev. Lett.* **1996**, *77*, 3371–3374.
34. Muller, F.; Hufner, S.; Sachdev, H.; Gsell, S.; Schreck, M. Epitaxial Growth of Hexagonal Boron Nitride Monolayers by a Three-Step Boration–Oxidation–Nitration Process. *Phys. Rev. B* **2010**, *82*, 075405.